Supporting Information

Covalent amide-bonded nanoflares for high-fidelity intracellular sensing and targeted therapy: a superstable nanosystem free of nonspecific interferences

Jiling Zhang,[†,1] Liangwei Lu,[†,1] Zhi-Ling Song,[†,] Wenjuan Song,[†] Zhuolin Fu,[†] Qiqi Chao,[†] Gao-Chao Fan,[†] Zhuo Chen,[‡,]* Xiliang Luo,[†,]**

[†]Key Laboratory of Optic-electric Sensing and Analytical Chemistry for Life Science, MOE, Shandong Key Laboratory of Biochemical Analysis, College of Chemistry and Molecular Engineering, Qingdao University of Science and Technology, Qingdao 266042, China

[‡]Molecular Science and Biomedicine Laboratory (MBL), State Key Laboratory of Chemo/Bio-Sensing and Chemometrics, College of Chemistry and Chemical Engineering and College of Life Sciences, Aptamer Engineering Center of Hunan Province, Hunan University, Changsha Hunan, 410082, China

[1]These authors contributed equally

Corresponding Author
**Email: zhilingsong@qust.edu.cn (Z. L. S.)*
**Email: xiliangluo@qust.edu.cn (X. L.)*
**Email: zhuochen@hnu.edu.cn (Z. C.)*

Table of Contents

1. Supplemental Materials and Methods

Reagents. Chloroauric (Ⅲ) acid tetrahydrate ($HAuCl_4·4H_2O$), ethanol, NaCl, $MgCl_2$, 16-mercaptohexadecanoic acid (MHA), sodium ascorbate, ethanol, diethylamine and tetraethyl orthosilicate (TEOS), were bought from Sinopharm Chemical Reagents Company (Shanghai, China). Trisodium citrate dihydrate ($C_6H_5Na_3O_7·2H_2O$), polyvinylpyrrolidone (PVP, Mw=40000), glutathione (GSH), bovine serum albumin (BSA), 1-ethyl-3-(3-dimethylaminopropyl) carbodiimide hydrochloride (EDC), 4-morpholineethanesulfonic acid (MES), HEPES (N-2-hydroxyethylpiperazine-N'-2-ethanesulfonic acid), chlorin e6 (Ce6), N-Hydroxysuccinimide (NHS) and 3-(4,5-dimethylthiazol-2-yl)-5(3-carboxymethoxyphenyl)-2-(4-sulfopheny)-2H-tetrazolium (MTS) were purchased from Sigma-aldrich. Deoxyribonuclease I (DNase I) were all obtained from Takara Biotechnology Co. Glutathione (GSH) were purchased from Adamas-beta. Graphene oxide (GO) were were obtained from Shanghai Titan Scientific. Penicillin streptomycin, Dulbecco's modified Eagle's medium (DMEM), Roswell Park Memorial Institute 1640 medium (RPMI-1640) and and fetal bovine serum (FBS) were obtained from Hyclone (Logan, UT, USA). Oligonucleotide sequences, TRIZOL reagent, miRNA First Strand cDNA Synthesis (Stem-loop Method) Kit and 2X SG Fast qPCR Master Mix (High Rox) Kit were bought from Sangon (Shanghai, China). 1,3-diphenylisobenzofuran (DPBF), 2',7'-dichlorofluorescein diacetate (DCFH-DA) and all other chemicals of analytical reagent grade were bought from Changsha Chemical Reagents Company (Changsha, China) and directly used as received without further purification. Doubly distilled water (resistance > 18 M Ω•cm) purified from a Milli-Q Integral System was used throughout all experiments.

Apparatus. Transmission electron microscopy (TEM, JEM-2010) was utilized to characterize the size and morphology. All UV-vis absorption spectra were recorded by UV-2600 spectrophotometer (Shimadzu). Raman spectroscopy were measured with Renishaw Invia Raman microscope with 633 nm excited laser. The absorbance in the MTS assay was gained on the Bio-Tek Multi-Mode Microplate Reader (Winooski, VT). Zeta potentials of the nanoparticles were determined at room temperature by a Zeta Plus Potential Analyzer (Brookhaven Instruments Corporation). A cytoFlex flow cytometer (Beckman Coulter) was used to perform all flow cytometric analysis. Centrifugation was carried out on a H1-16KR (KeCheng, China). Fluorescence confocal images were recorded by Olympus FV1000. Fluorescence spectra were acquired with an F-7000 fluorescence spectrophotometer (Hitach, Japan).

Synthesis of AuNPs. To ensure the uniformity of Au@graphene (AuG) NPs, the core models, Au nanoparticles (AuNPs) with a diameter of ~25 nm, were first synthesized by the typical sodium citrate reduction method.[S1] 100 mL of 0.01% (w/v) $HAuCl_4$ solution was boiled with vigorous stirring, and 2.7 mL of 1% (w/v) trisodium citrate solution was quickly added to the boiling solution. When the solution turned deep red, indicating the formation of Au NPs, the solution was stopped stirring and cooled down. Then the obtained AuNPs were collected by centrifugation (8000 rpm, 10 min) and re-dispersed in ultrapure water after washing with water several times. Finally, AuNPs colloid was stored at 4 ℃ for the further experiments, which concentration was calculated according to the Uv-vis absorbance intensity at 450 nm based on the Lambert-Beer law.

Synthesis of Au@SiO_2 NPs. Before graphene growth, the AuNPs were coated with porous SiO_2 isolation shells to separate the surfaces and eliminate the gathering of molten Au at high temperature. The coating of SiO_2 shell on the AuNPs was performed according to the previous report[S2] with a little modification. First of all, 10 mL of AuNP solution was mixed with 30 mL ethanolic solution of 16-mercaptohexadecanoic acid (MHA) (2 mM) for 10 min at room temperture. Then, 3 mL of diethylamine and 10 μL tetraethyl orthosilicate (TEOS) were slowly added into the mixed solution under stirring and reacted for 40 min at room temperature. Then the obtained Au@SiO_2 NPs were collected by centrifugation (8000 rpm, 10 min) and re-dispersed in methanol after washing with water and ethanol for several times.

Anti-interference assays. For comparation, the molecular probe ROx-rcDNA-BHQ, Au-S bonded nanoprobe ROX-rcDNA-Au, and π-π bonded nanoprobe ROX-cDNA-GO were all synthesized. The nuclease stability was investigated by monitoring the fluorescence of ROx-rcDNA-BHQ and ROX-rcDNA-AuG in the absence or presence of DNase I (5 U/L) for 120 min. The nuclease stability was investigated by monitoring the fluorescence of ROx-rcDNA-BHQ and ROX-rcDNA-AuG in the absence or presence of DNase I (5 U/L) for 120 min. The capability to resist glutathione (GSH) was evaluated by monitoring the fluorescence of ROX-rcDNA-Au and ROX-rcDNA-AuG in the absence or presence of GSH (5 mM) for 8 h. Similarly, the capability to resist single-stranded interfering DNA (iDNA) was assessed by monitoring the fluorescence of ROX-cDNA-GO and ROX-rcDNA-AuG in the absence or presence of iDNA (0.5 μM) for 120 min. All the results indicated that our covalent system ROX-rcDNA-AuG possessed a better resistance to the interfering species.

In vitro Detection. 80 μL ROX-rcDNA-AuG nanoprobes were mixed with 20 μL HEPES solution containing different concentrations of miR-21. After incubation at 37 ℃ for 40 min, the fluorescence spectra were detected by an F-7000 fluorescence spectrophotometer. The adopted excitation/emission wavelength was 580/610 nm.

Cell culture. MCF-7 and HEK-293 T cells were cultured in DMEM containing 10% premium fetal bovine serum (FBS) and 1% penicillin-streptomycin. HeLa cells were cultured in RPMI 1640 medium supplemented with 10% premium fetal bovine serum (FBS) and 1% penicillin-streptomycin. All cells were maintained at 37 °C with 5% CO_2 in a humidified atmosphere

Cytotoxicity test. Good biocompatibility is a vital attribute for an intracellular nanoprobe. We investigated the cytotoxicity of the ROX-rcDNA-AuG nanoprobe in different concentrations for the MCF-7 cells by MTS assay. The cell viability measurement was evaluated based on the reduction of MTS to formazan crystals by the mitochondrial dehydrogenases. 1×10^3 MCF-7 cells in 50 μL washing buffer (Dulbecco`s phosphate buffered saline, DPBS, Gibco) were pre-seeded to each test well in 96-well plate and then incubated with PRMI-1640 culture medium for 24 h.Next, the culture medium was taken out and fresh culture medium with different concentrations of nanoprobes (0-100 μg mL^{-1}) was added. The cells were incubated for 24 h and then 100 μL fresh PRMI-1640 medium and 20 μL MTS solution were added into each well and incubated for another 0.5 h. Finally, the absorbance intesity at 490 nm was recorded by a Bio-Tek Multi-Mode Microplate Reader (Winooski, VT) to assess the cell viability. All the experiments were conducted at least 3 times.

Fluorescence sensing in living cells. For the fluorescence imaging of living cells, ROX-rcDNA-AuG nanoprobes were incubated with MCF-7 (positive cell, over-express miR-21), Hela (positive cell, over-express miR-21) and HEK-293T (negative cell, low-express miR-21) respectively in 10% FBS-containing culture medium for 3 h at 37℃. Then cell imaging was analyzed at scanning confocal microscope under a 543 nm laser, and emissions were recorded in the red channel.

Inhibitor transfection. miR-21 inhibitor transfection was performed using Lipofectamine 3000 reagent (Invitrogen) with a little modification according to the protocol provided by the manufacturer. Briefly, Lipofectamine 300 (5 μL) and miR-21 inhibitors (2 nmol) were incubated separately in Opti-MEM media (Invitrogen) for 3 minutes at room temperature. Then these two solutions were mixed and allowed to incubate for an additional 25 minutes to form inhibitor-Lipofectamine complex. Next, the prepared inhibitor-Lipofectamine complex was mixed with DMEM without FBS or antibiotics and added into MCF-7 cells. After incubation for 4 hours, cells were washed several times with DPBS and covered with DMEM without FBS or antibiotics.

Quantitative reverse transcription-PCR (qRT-PCR) analysis. The miR-21 gene expressions levels in three types cells of MCF-7, HeLa and HEK 293T were confirmed by RT-PCR. Primers were designed and synthesized by Sangon (Shanghai, China) and the primer sequences were listed in Table S2. Total RNA was isolated from iced cell lysis buffer using TRIZOL reagent according to the protocol provided by the manufacturer. The cDNAs were reverse-transcribed using the miRNA First Strand cDNA Synthesis (Stem-loop Method) Kit according to the manufacturer's instructions. qRT-PCR was performed using 2X SG Fast qPCR Master Mix (High Rox) Kit on an ABI Stepone real-time PCR system. Fluorescent dye used in RT-PCR reactions was SYBR Green I. Briefly, the RT-PCR cycles were conducted to 45 cycles for amplification of miR-21. The reaction mixture was incubated at 95 ℃ for 3 min, followed by 40 cycles of 95 ℃ for 30 s and 60 ℃ for 30 s, 72 ˚C for 30 s. For melting curve analysis, fluorescence signals were collected continuously from 72°C to 95°C at 0.3 °C per second. The relative expression levels of the miR-21 were analyzed using a comparative threshold cycle ($2^{-\Delta\Delta Ct}$) method. The expression of the non-coding small nuclear RNA U6 was used as endogenous control for each sample.

Chlorin e6 (Ce6). Each Ce6 molecule has three carboxyl groups (**Figure S16**), which may be conjugated with the amino group at the 3'- end of the DNA product. The PDT therapy mechanism of Ce6 is based on the formation of reactive oxygen species (ROS), an aggressive chemical species. When irradiated by visible red light (660-nm laser), the photosensitizer (Ce6) transfers the light energy to tissue oxygen (O_2), eventually producing ROS. The ROS can rapidly oxidize the cellular biomolecules, including amino acids, cholesterol and unsaturated fatty acids, and further causes membrane damage, ultimately leading to cell death.[S3,S4]

Synthesis of Ce6-rDNA. The modification of Ce6 drug molecules onto amino-labeled rDNA (NH_2-rDNA) was performed according to the previous report[S5] with a little modification. 10

μmol of Ce6 molecules were mixed with equivalent EDC and NHS and then dissolved in 250 μL of DMF to form a transparent solution. After incubation for 30 minutes, Ce6 molecules were activated. Then, 1 μmol of NH_2-rDNA pre-dissolved in 250 mL, 0.1 M of $NaHCO_3$ was added into the above DMF solution and stirred for 24 h at room temperature. The obtained solution was purified by dialysis (MW 2000 Da) for 3 days. On the first day, 0.1 M $NaHCO_3$ was used as the dialysis solution to remove residual Ce6 molecules, and then $NaHCO_3$ was replaced with deionized water for the next 2 days. Then, the Ce6-rDNA were collected through a vacuum dryer and further purified by reversed-phase HPLC.

Fabrication of Ce6-rcDNA-AuG nanosystem. cDNA-AuG NPs (200 μg mL^{-1}) were incubated with Ce6-rDNA (final concentration 0.5 μM) solution at 37 °C for 1 h in HEPES buffer under continuous stirring. After the hybridization of cDNA and rDNA, the mixture was treated with 5 μM single-stranded bDNA for 30 min to replace the physically adsorbed rDNA sequences. Finally, the Ce6-rcDNA-AuG nanoprobe was washed three times with the HEPES buffer and stored at 4 °C for the further experiments.

Detection of $^1O_2$ generation in vitro. As the production of singlet oxygen ($^1O_2$) is very important for PDT to kill cancer cells, we investigated the $^1O_2$ generation capability of Ce6-rcDNA-AuG with miR-21 by using 1,3-diphenylisoben-zofuran (DPBF) as a probe. Ce6-rcDNA-AuG (100 μg mL^{-1}), H_2O_2 (2 mM) and DPBF (0.02 mM) was added into PBS buffer (pH 7.0). The DPBF absorption peak at 420 nm was recorded by UV-Vis spectrophotometer at 0, 4, 8, 12, 16, and 30 min after irradiation with 660 nm laser (0.65 W cm^{-2}).

Detection of intracellular $^1O_2$ generation. Briefly, MCF-7 cells (positive cell, over-express miR-21) were incubated at 37 °C under 5% CO_2 for 24 h. Then, MCF-7 cells were incubated with Ce6-rcDNA-AuG (100 μg mL^{-1}) for 3 h in 10% FBS-containing culture medium. After washing 3 times with PBS, the cells were exposed to 660 nm laser (0.65 W cm^{-2}) for 30 min. Then the 2′, 7′-dichlorodihydrofluorescein diacetate (DCFH-DA) was added into cells and the mixture was incubated for 20 min at 37 °C. Then cell imaging was analyzed at confocal microscope under 488 nm laser, and emissions were recorded in the green channel.

Supplementary Figures

Table S1. DNA sequences used in this study.

Oligonucleotide	**Sequences (from 5' to 3')**
Capture DNA (cDNA)	TAGCTTATCAGA CTG
COOH-cDNA	COOH-TAGCTTATCAGACTG
HS-cDNA	HS-TAGCTTATCAGACTG
BHQ-cDNA	BHQ2-TAGCTTATCAGACTG
miR-21	UAGCUUAUCAGACUGAUGUUGA
miR-21 inhibitor	UmCmAmAmCmAmUmCmAmGmUmCmUmGmAmUmAmAmGmCmUmAm[a]
Recognition DNA of miR-21 (rDNA)	TCAACATCAGTCTGATAAGCTA
ROX-rDNA	TCAACATCAGTCTGATAAGCTA-ROX
NH_2-rDNA	TCAACATCAGTCTGATAAGCTA-NH_2
Ce6-rDNA	TCAACATCAGTCTGATAAGCTA-Ce6
Blocking DNA (bDNA)	AAAAAAAAAAAAAAAAAAAAAAAAAAAAAA
Interfering DNA (iDNA)	TAGCAGCACGTAAATATTGGCG
miR-16	UAGCAGCACGUAAAUAUUGGCG
miR-141	UAACACUGUCUGGUAAAGAUGG
miR-630	AGUAUUCUGUACCAGGGAAGGU
miR-203	GUGAAAUGUUUAGGACCACUAG
miR-200b	AAUACUGCCUGGUAAUGAUGA

[a]m is 2'-O-methyl.

Table S2. The primers used for qRT-PCR analyses in this study.

Primer	**Sequences (from 5' to 3')**
U6 forward	CTCGCTTCGGCAGCACA
U6 reverse	AACGCTTCACGAATTTGCGT
miR-21 RT	GTCGTATCCAGTGCAGGGTCCGAGGTATTCGCACTGGATACGACTCAACA
miR-21 forward	GCGCGTAGCTTATCAGACTGA
miR-21 reverse	AGTGCAGGGTCCGAGGTATT

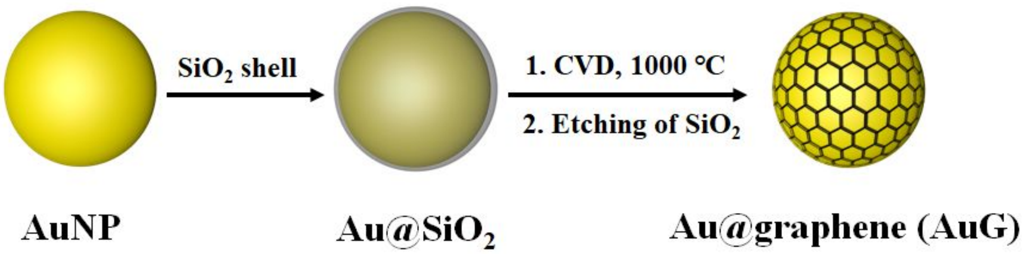

Figure S1. The synthesis of AuG NP.

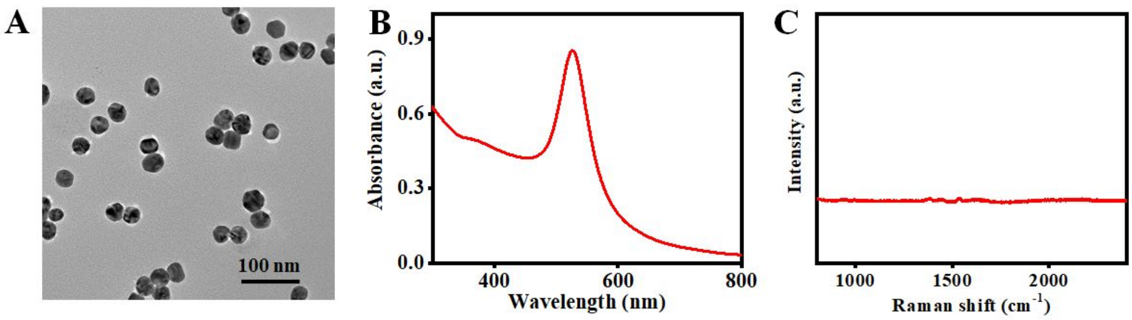

Figure S2. Characterization of AuNPs. (A) TEM images of AuNPs. (B) UV-vis spectrum of AuNPs solution. (C) Raman spectrum of AuNPs solution.

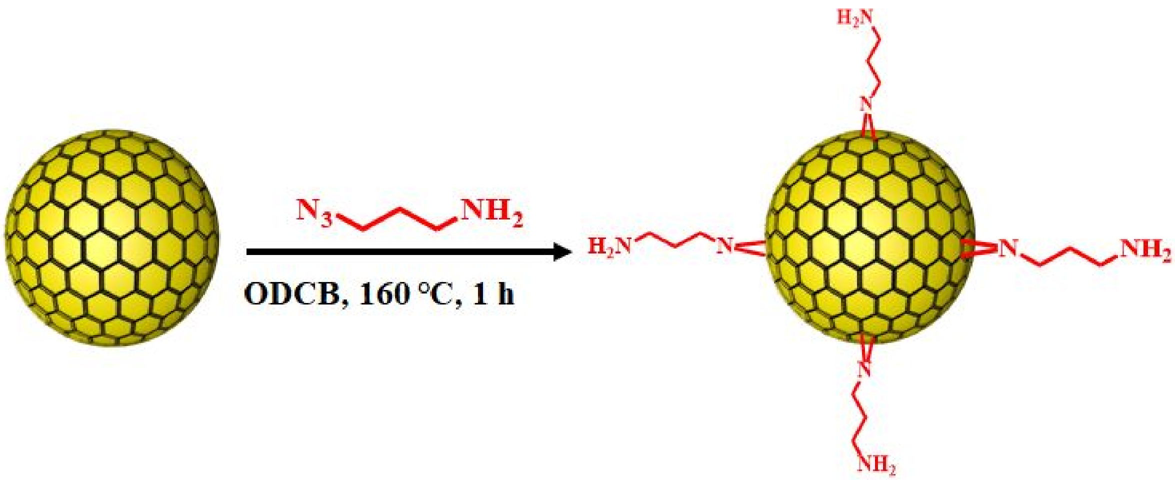

Figure S3. The synthesis of the amino-functionalized AuG (NH_2-AuG) NP.

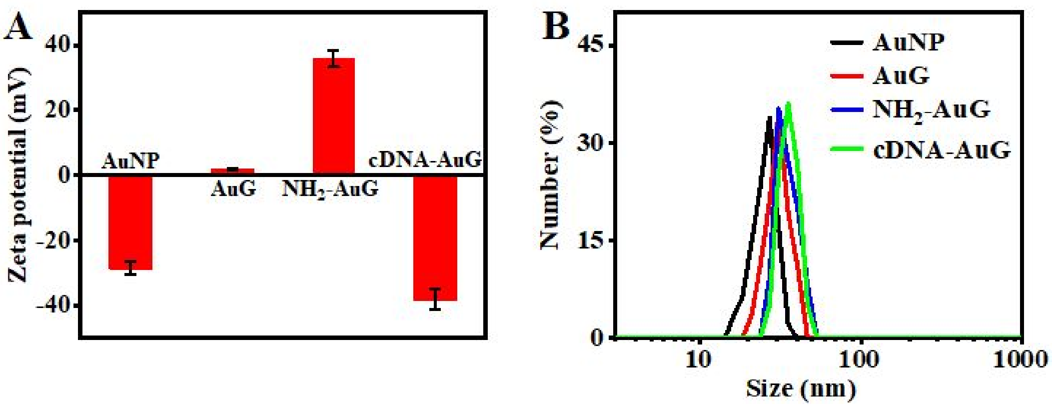

Figure S4. (A) Zeta potentials and (B) hydrodynamic size characterizations of AuNP, AuG, NH_2-AuG and cDNA-AuG.

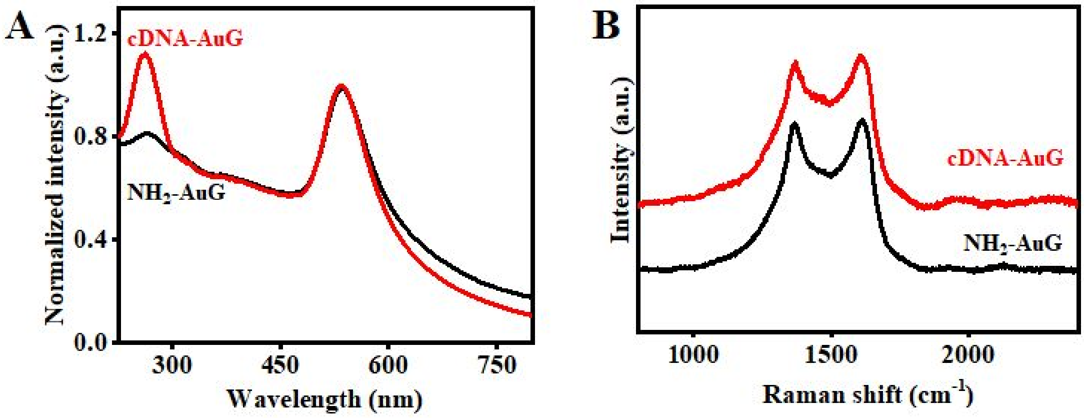

Figure S5. UV-vis (A) and Raman (B) characterizations of NH_2-AuG (black) and cDNA-AuG (red).

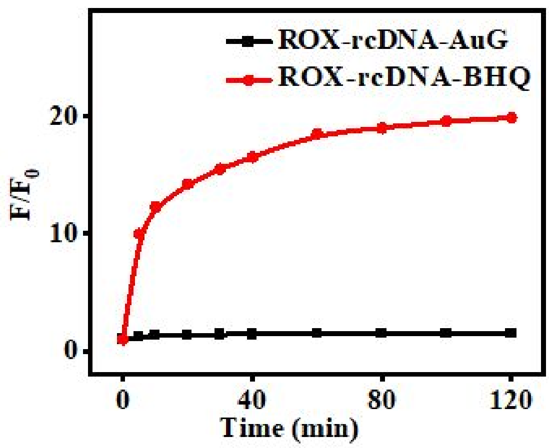

Figure S6. Fluorescence analysis of the stability of free DNA probe (ROX-rcDNA-BHQ) and covalent nanoprobe (ROX-rcDNA-AuG) in 10% FBS. These results demonstrates that the free DNA probe is easily degraded by FBS, while the covalent nanoprobe shows high stability.

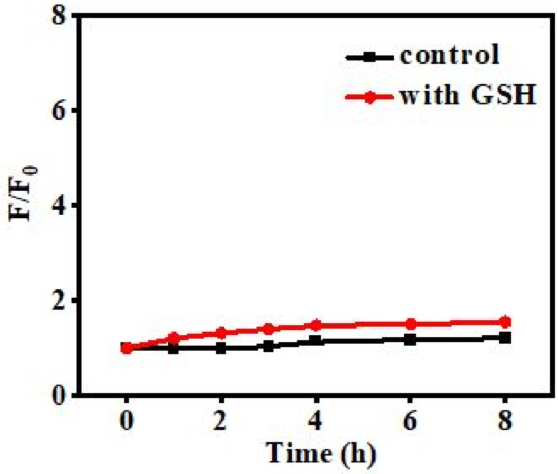

Figure S7. Fluorescence stabilities of covalent nanosystem (ROX-rcDNA-AuG) in presence of high concentration of GSH (10 mM).

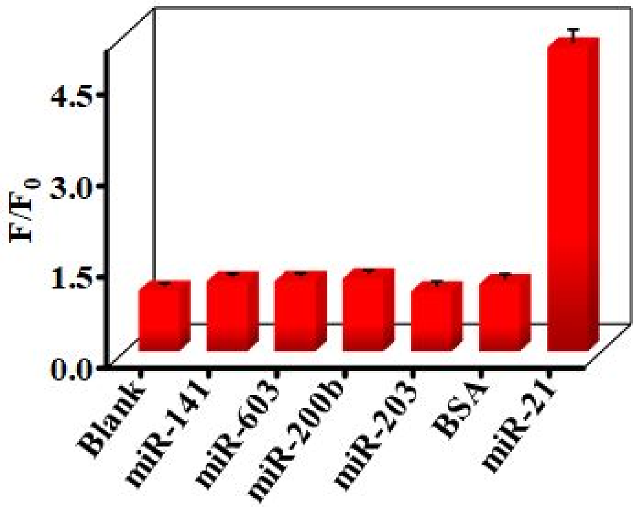

Figure S8. Specificity of the ROX-rcDNA-AuG nanoprobe. All of the miRNAs were at 100 nM, and the BSA was at 10 mM.

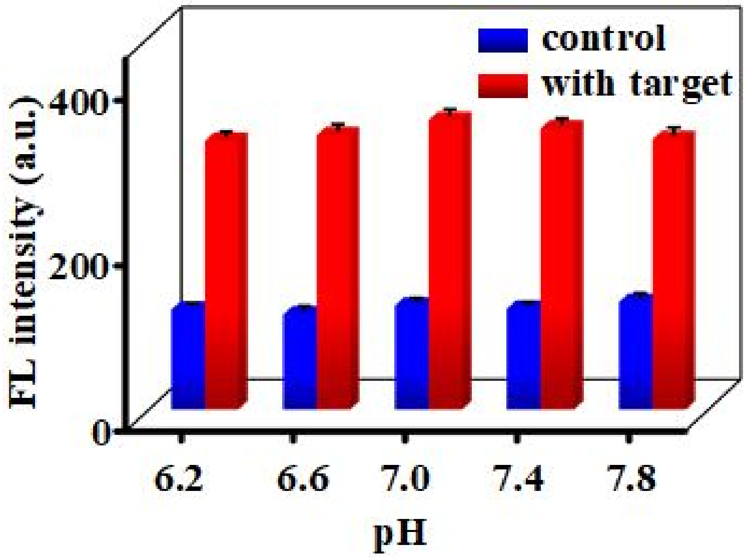

Figure S9. Fluorescence intensity changes of the ROX-rcDNA-AuG nanoprobe at different pH values in the absence (blue) and presence (red) of miR-21 (10 nM).

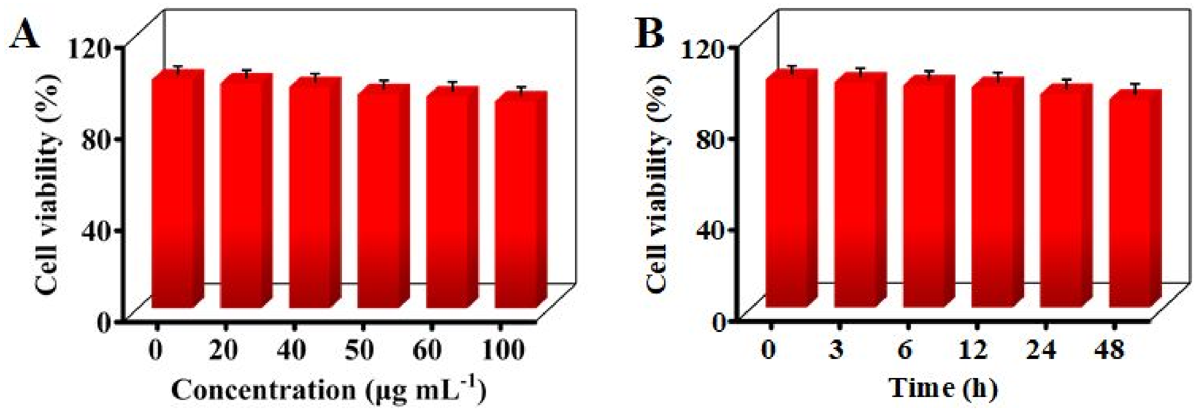

Figure S10. (A) Cell viability of MCF-7 cells treated with different concentrations (0-100 μg mL^{-1}) of ROX-rcDNA-AuG nanoprobe for 24 h. (B**)** Cell viability of MCF-7 cells after incubation with 50 μg mL^{-1} ROX-rcDNA-AuG nanoprobe for various time.

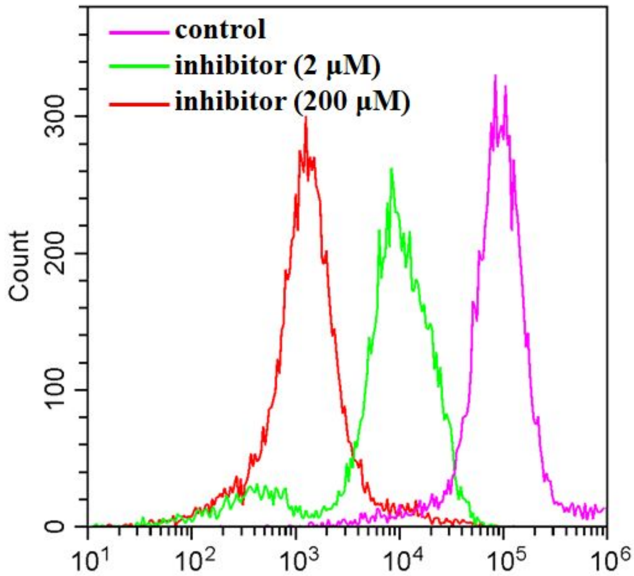

Figure S11. Flow cytometry analysis of miR-21 inhibitor-pretreated MCF-7 cells after incubation with ROX-rcDNA-AuG nanoprobes. The concentrations of miR-21 inhibitor are 0 (pink), 2 μM (green) and 200 μM (red), respectively.

Table S3. Average Ct values in RT-PCR assay of miR-21 in inhibitor-pretreated MCF-7 cells

Inhibitor (μM)	**miR-21**	**U6**	**ΔCt**	**ΔΔCt**	$2^{-\Delta\Delta Ct}$
0	20.868	16.742	4.126	-6.258	76.532
2	22.982	17.568	5.414	-4.97	31.341
200	26.767	16.383	10.384	0	1

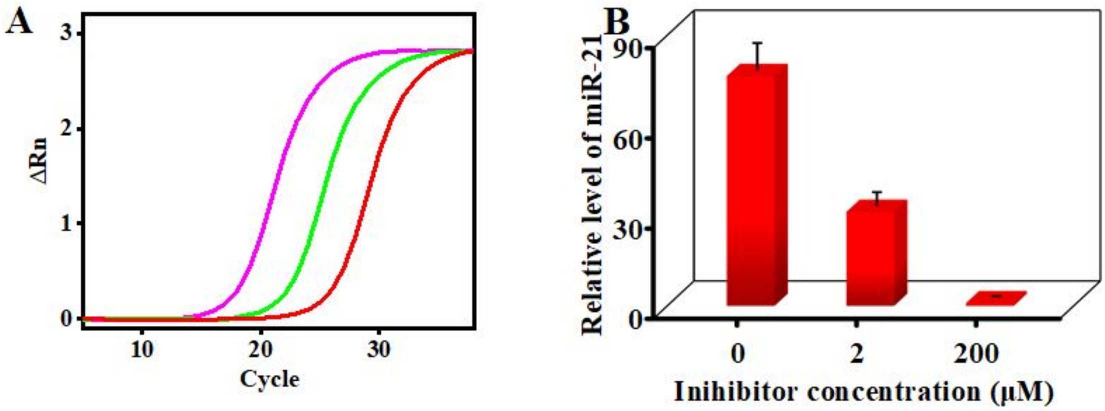

Figure S12. Quantitative reverse transcription-PCR (qRT-PCR) analysis of miR-21 in the miR-21 inhibitor-pretreated MCF-7 cells. (A) Real-time fluorescence curves in qRT-PCR analysis. The concentrations of miR-21 inhibitor are 0 (pink), 2 μM (green) and 200 μM (red), respectively. (B) Relative expression levels for miRNA-21.

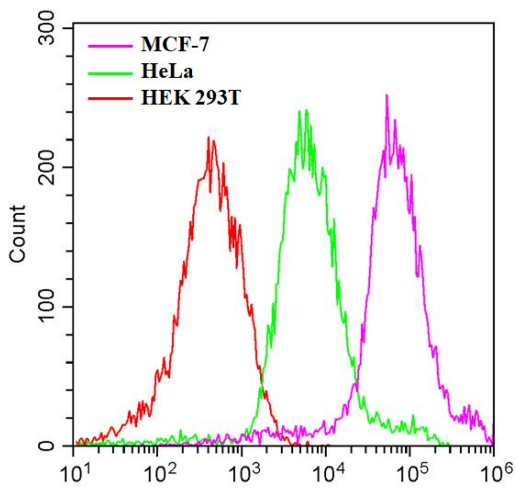

Figure S13. Flow cytometry analysis of different cells treated with ROX-rcDNA-AuG nanoprobes, including MCF-7 cancer cells, HeLa cancer cells and HEK 293T normal cells.

Table S4. Average Ct values in RT-PCR assay of miR-21 in different cell lines.

Cell line	miR-21	U6	ΔCt	ΔΔCt	$2^{-\Delta\Delta Ct}$
MCF-7	20.868	16.742	4.126	-7.401	169.014
HeLa	21.437	15.266	6.171	-5.356	40.956
HEK 293T	27.819	16.292	11.527	0	1

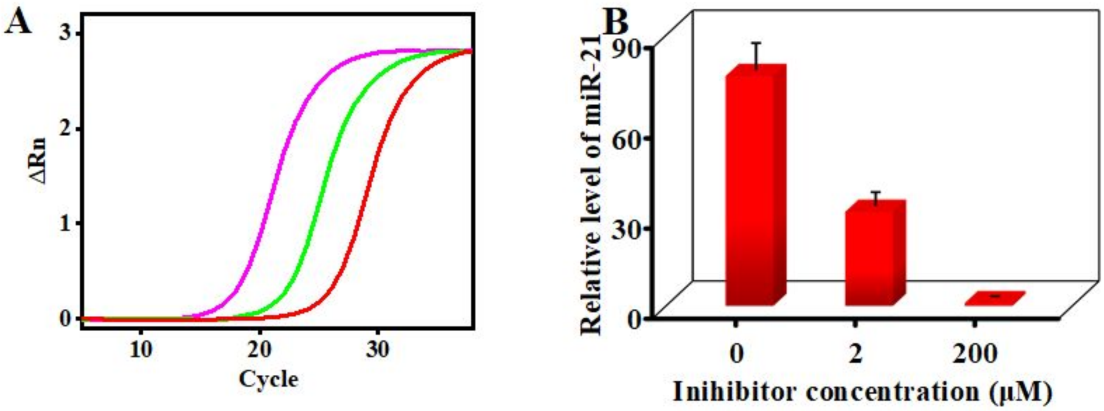

Figure S14. Quantitative reverse transcription-PCR (qRT-PCR) analysis of miR-21 in the three different cell lines. (A) Real-time fluorescence curves of MCF-7 (pink), HeLa (green) and HEK 293T (red) cells in qRT-PCR analysis. (B) Relative expression levels for miRNA-21.

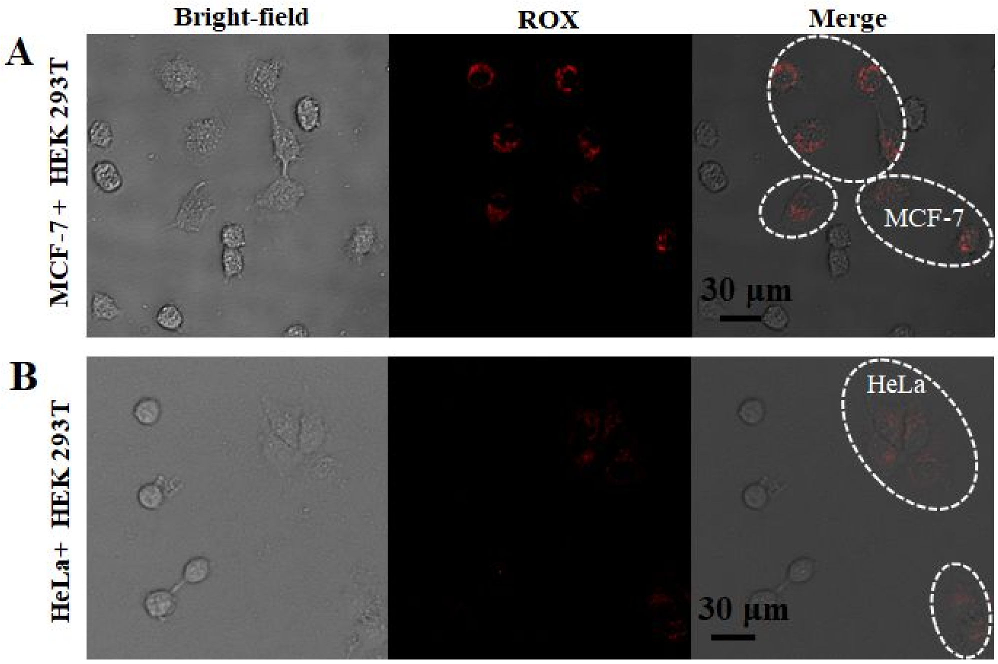

Figure S15. miR-21-triggered confocal images in the mixed cells after incubation with ROX-rcDNA-AuG nanoprobes. (A) MCF-7 cancer cells and HEK 293T normal cell. The circles depict the MCF-7 cancer cells. (B) HeLa cancer cells and HEK 293T normal cell. The circles depict the HeLa cancer cells.

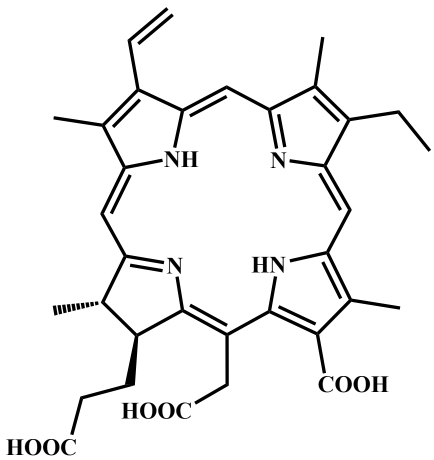

Ce6

Figure S16. Chemical structure of Ce6 molecule.

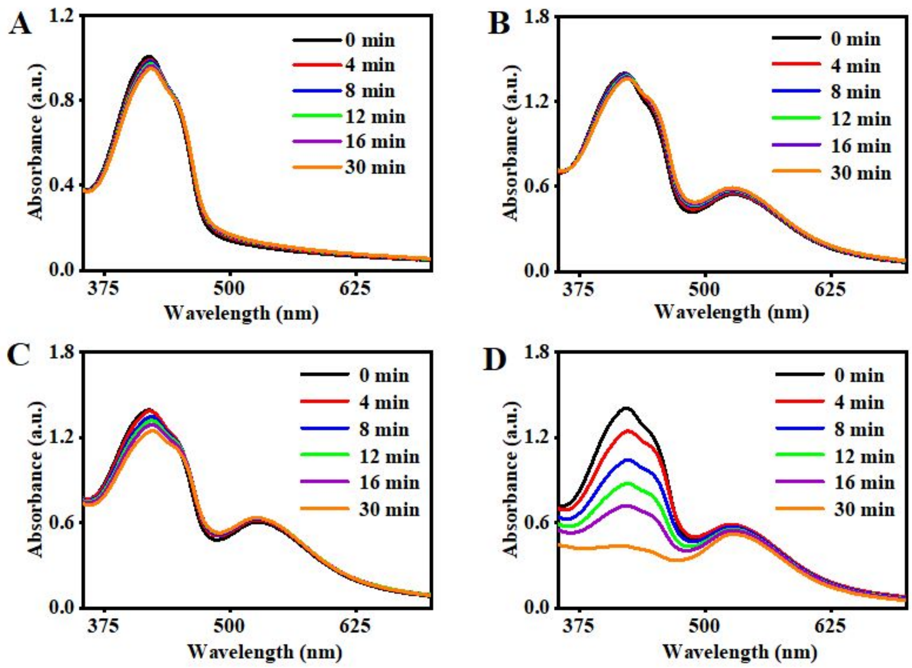

Figure S17. (A) UV-Vis absorption spectra of DPBF after irradiation for different times with 660 nm laser. (B) Absorption spectrum changes of DPBF under laser irradiation with treatment of AuG. (C) Absorption spectrum changes of DPBF under laser irradiation with Ce6-rcDNA-AuG in the absence of miR-21. (D) Absorption spectrum changes of DPBF under laser irradiation with Ce6-rcDNA-AuG in the presence of miR-21.

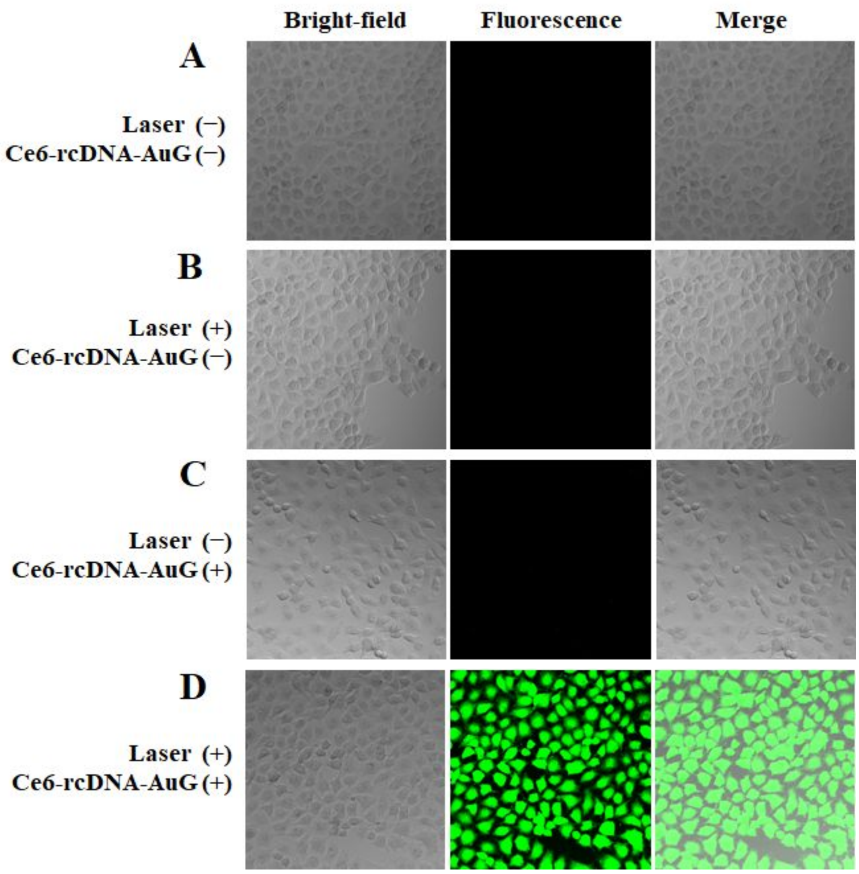

Figure S18. Confocal fluorescence images of singlet oxygen generation in MCF-7 cells detected by using using 2',7'-dichlorofluorescein diacetate (DCFH-DA, ROS fluorescent label). (A) Control MCF-7 cells without treatment of Ce6-rcDNA-AuG and laser irradiation. (B) MCF-7 cells with only laser irradiation. (C) MCF-7 cells treated with only Ce6-rcDNA-AuG. (D) MCF-7 cells treated with Ce6-rcDNA-AuG and laser irradiation. Upon irradiation with 660 nm laser, the ROS generation of Ce6-rcDNA-AuG can oxidize DCFH, a nonfluorescent part of DCFH-DA, to 2',7'-dichlorofluorescein and emit bright green fluorescence in cells. The Green fluorescence represents intracellular ROS production

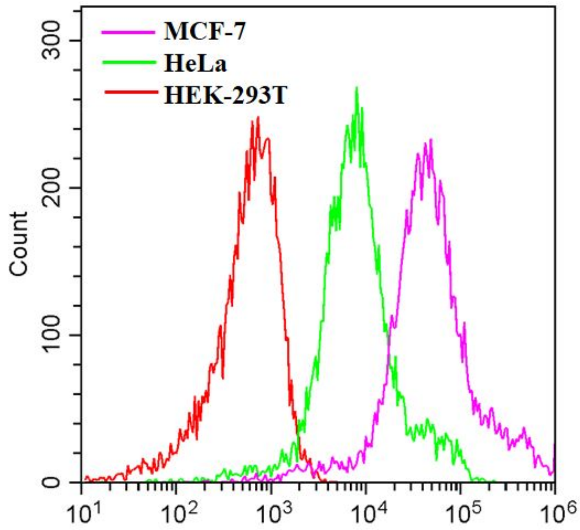

Figure S19. Flow cytometry analysis of different cells treated with Ce6-rcDNA-AuG nanoprobes, including MCF-7 cancer cells, HeLa cancer cells and HEK 293T normal cells.

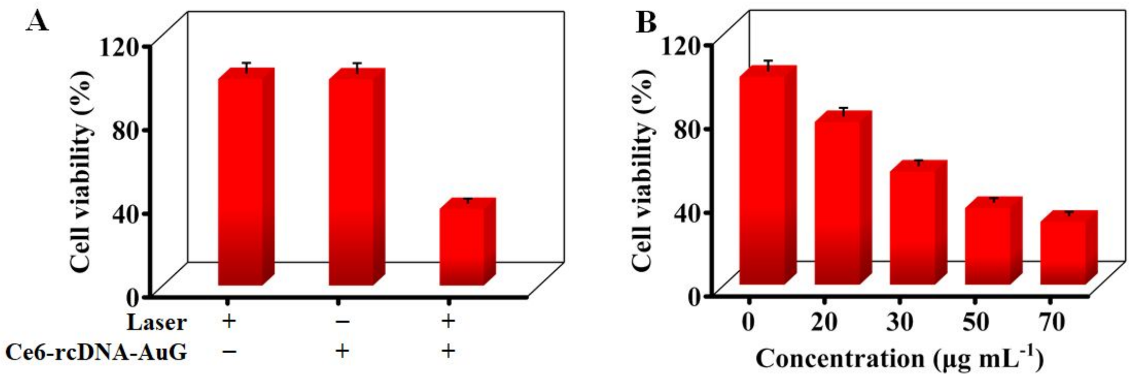

Figure S20. (A) The cell viability of MCF-7 under different treatments. (B) Cell viability of MCF-7 cells treated with different concentrations of Ce6-bcDNA-AuG nanoprobe after irradiation of 660 nm (0.65 W/cm^2) light for 30 min.

Table S5. Comparison of this assay with other anti-interference systems.

Nanosystem	Cancer therapy	Fluorescence label, other specials	Modified DNA or peptide	Anti-interference species	Target (LOD[b])	Ref.
FRET Nanoflare	--	Two, FRET dyes	HS-DNA, Hairpin DNA	GSH, Dnase I	TK1 mRNA (--[a])	14
Au-S nanoflare	--	One, -[d]	Se-peptide	GSH	Casapase-9 (--)	12
FRET nanoflare	--	Two, FRET dyes	HS-DNA, PC-DNA[c]	--	let-7a miRNA (2.3 nM)	11
DNA/GO	--	Three, FRET dyes, one quencher	DNA	BSA, nucleic acid	miR-21 (0.44 nM)	38
covalent nanoflare	Yes	One, -	NH_2-DNA	GSH, Dnase I, nucleic acid	miR-21 (0.066 nM)	This work

[a] not mentioned

[b] detection limit

[c] a DNA containing a group of photocleavable linkers

(PC-linkers)

[d] needing no special (applicable for usual fluorescence dyes)

[e] graphene oxide

References:

1. Ziegler, C.; Eychmüller, A. Seeded growth synthesis of uniform gold nanoparticles with diameters of 15-300 nm. *J. Phys. Chem. C* **2011**, *115*, 4502-4506.
2. Bai, Y.; Gao, C.; Yin, Y. Fully alloyed Ag/Au nanorods with tunable surface plasmon resonance and high chemical stability. *Nanoscale* **2017**, *9*, 14875-14880.
3. Zhu, Z.; Tang, Z.; Phillips, J. A.; Yang, R.; Wang, H.; Tan, W. Regulation of singlet oxygen generation using single-walled carbon nanotubes. *J. Am. Chem. Soc.* **2008**, *130*, 10856-10857.
4. Narumi, A.; Rachi, R.; Yamazaki, H.; Kawaguchi, S.; Kikuchi, M.; Konno, H.; Osaki, T.; Okamoto, Y.; Shen, X.; Kakuchi, T.; Kataoka, H.; Nomoto, A.; Yoshimura, T.; Yano, S. Maltotriose-Chlorin e6 conjugate linked via tetraethyleneglycol as an advanced photosensitizer for photodynamic therapy. synthesis and antitumor activities against canine and mouse mammary carcinoma cells. ACS Omega **2021**, *6*, 7023-7033
5. You, M.; Zhu, G.; Chen, T.; Donovan, M. J.; Tan, W. Programmable and multiparameter DNA-based logic platform for cancer recognition and targeted therapy. *J. Am. Chem. Soc.* **2015**, *137*, 667-674.